



Design of a fixed-order RST controller for interval systems : application to the control of piezoelectric actuators.

Sofiane Khadraoui, Micky Rakotondrabe, Philippe Lutz

► To cite this version:

Sofiane Khadraoui, Micky Rakotondrabe, Philippe Lutz. Design of a fixed-order RST controller for interval systems : application to the control of piezoelectric actuators.. Asian Journal of Control, 2013, 15, pp.142-153. hal-00905248

HAL Id: hal-00905248

<https://hal.science/hal-00905248>

Submitted on 21 Nov 2013

HAL is a multi-disciplinary open access archive for the deposit and dissemination of scientific research documents, whether they are published or not. The documents may come from teaching and research institutions in France or abroad, or from public or private research centers.

L'archive ouverte pluridisciplinaire **HAL**, est destinée au dépôt et à la diffusion de documents scientifiques de niveau recherche, publiés ou non, émanant des établissements d'enseignement et de recherche français ou étrangers, des laboratoires publics ou privés.

Design of a fixed-order RST controller for interval systems: application to the control of piezoelectric actuators

Sofiane Khadraoui, Micky Rakotondrabe and Philippe Lutz

ABSTRACT

This paper presents a technique for designing a robust polynomial RST controller for parametric uncertain systems. The uncertain parameters are assumed to be bounded by intervals. The computation of the controller is addressed by introducing the interval arithmetic. The controller synthesis is formulated as a set inversion problem that can be solved using the SIVIA algorithm. The proposed method is afterwards applied to design a robust controller for a piezoelectric microactuator. The experimental results show the efficiency of the proposed method. Finally, a fine stability analysis is performed to analytically prove the robustness of the designed controller.

Key Words: Parametric uncertainty, interval model, robust performance, RST controller design, piezoelectric microactuators.

I. Introduction

During the last decade, the problem of designing robust control laws for parametric uncertain systems has attracted much attention [1, 2, 3, 4, 5, 6, 7, 8, 9]. Practical considerations have motivated the study of control systems with unknown but bounded parameter uncertainties. Indeed, these uncertainties are often due to various factors such as the sensitivity to environmental conditions (vibrations, evolution of ambient temperature, etc.), nonlinearities (hysteresis, time varying parameters, creep, etc.), sensor limitations and un-modelled dynamics of systems [1, 5, 6]. If not considered, these uncertainties cause the degradation of the closed-loop performances or the loss of stability. It is therefore necessary to take them into account and to incorporate enough robustness to the controller in order to maintain the nominal performances.

The compensation of these parametric uncertainties is often accomplished by means of adaptive control [9, 10] or by means of robust control laws such as H_2 , H_∞ and μ -synthesis [12, 13]. The adaptive control methods require a precise model which is difficult to obtain. Concerning the robust H_2 , H_∞ and μ -synthesis approaches, their efficiency is proved in several applications (Single input single output (SISO) and multiple input multiple output (MIMO) systems) while their major disadvantage is the derivation of high-order controllers which are time consuming and which limit their embedding possibilities, particularly for embedded microsystems. One way to represent parametric uncertainties is to let each parameter take its value within a range called interval [3, 4, 14]. In addition to the natural way and simplicity of using intervals to bound uncertain parameters, interval arithmetic presents a symbolic or a numeric certificate of the results. Thus, using interval arithmetic for modeling and control design leads to certified robust stability and performances if a solution exists. For instance, the stability analysis of a characteristic polynomial subjected to uncertain parameters has been discussed in many works

Manuscript received April, 2011. This work is supported by the Conseil General du Doubs.

FEMTO-ST Institute, UMR CNRS 6174-UFC/ENSM/UTBM, Automatic Control and Micro-Mechatronic Systems depart., AS2M, 24 rue Alain Savary, Besançon 25000, France.

[3, 15, 16]. It was often based on the Routh's criteria and/or on the Kharitonov's theorem. The work in [11] presents the stability of uncertain systems with interval time-varying delay. Reference [17] discusses an approach to design robust stabilizing controllers for interval systems in the state-space representation. A systematic computational technique to design robust stabilizing controllers for interval systems using the constrained optimization problem was proposed in [18]. While the above works consider robust stability, robustness on performances for interval systems has also been discussed in several works [22, 4, 19, 20, 21, 23]. The work in [22] presents an interesting result on the inclusion of interval system performances. Reference [19] proposed a prediction-based control algorithm and its application to a welding process modelled by intervals. In [20], a state feedback controller was first considered to ensure the robust stability, then a pre-filter that guarantees the required performances was constructed by applying a curve fitting technique. In [21], an approach to design a robust proportional-integral-derivative (PID) controller for interval transfer function was derived. However the method was limited to 2nd order uncertain systems. In our previous work [23], we proposed to extend the method for n^{th} order uncertain systems but still with zero-order numerator. However, the order of the derived controller was not *a priori* fixed and thus might not adapt to the hardware for implementation in embedded microsystems.

In this paper, we propose the interval modeling of a generalized n^{th} order uncertain parameter (without restriction on the numerator's order), and the design of a robust fixed-order controller to ensure specified performances. The robust controller considered in this contribution is a polynomial *RST* controller. The polynomials R and S allow creation of a feedback control in order to be robust to the uncertainties, while the polynomial T is introduced in the feedforward to improve the tracking. The computation of these polynomials is based on the inclusion performances theorem [22]. The main advantages of the proposed method relative to existing works are: i) no restriction is imposed on the system order; ii) and the order of the controller is *a priori* fixed, thus low-order (robust) controllers can be yielded. Furthermore, the suggested approach in this paper is simple and involves less computational complexity. The controller synthesis problem is formulated as a

set-inversion problem defined as the inclusion parameter by parameter.

The paper is organized as follows. In Section II, preliminaries related to interval arithmetic and systems are recalled. Section III is dedicated to the computation of the controller using the proposed approach. In Section IV, we apply the proposed method to model and control piezoelectric actuators. The experimental results and discussion are presented in Section V. Finally, to evaluate the robustness of the implemented controller, a closed-loop stability analysis is presented in Section VI.

II. Interval analysis preliminaries

2.1. Definition of interval

An interval $[x]$ can be defined by the set of all real numbers given as follows:

$$[x] = [x^-, x^+] = \{x \in \mathbb{R} / x^- \leq x \leq x^+\} \quad (1)$$

x^- and x^+ are the left and right endpoints respectively. $[x]$ is degenerate if $x^- = x^+$.

The width of an interval $[x]$ is given by:

$$width([x]) = x^+ - x^- \quad (2)$$

The midpoint of $[x]$ is given by:

$$mid([x]) = \frac{x^+ + x^-}{2} \quad (3)$$

The radius of $[x]$ is defined by:

$$rad([x]) = \frac{x^+ - x^-}{2} \quad (4)$$

2.2. Operations on intervals

The result of an operation between two intervals is an interval that contains all possible solutions as follows. Given two intervals $[x] = [x^-, x^+]$, $[y] = [y^-, y^+]$ and $\circ \in \{+, -, \cdot, /\}$, we can write:

$$[x] \circ [y] = \{x \circ y \mid x \in [x], y \in [y]\} \quad (5)$$

Therefore, the sum of two intervals $[x] + [y]$ is given by:

$$[x] + [y] = [x^- + y^-, x^+ + y^+] \quad (6)$$

the difference of two intervals $[x] - [y]$ is:

$$[x] - [y] = [x^- - y^+, x^+ - y^-] \quad (7)$$

the product of two intervals $[x].[y]$ is:

$$[x].[y] = [\min(x^-y^-, x^-y^+, x^+y^-, x^+y^+), \max(x^-y^-, x^-y^+, x^+y^-, x^+y^+)] \quad (8)$$

and finally, the quotient $[x]/[y]$ is given by

$$[x]/[y] = [x].[1/y^+, 1/y^-], 0 \notin [y] \quad (9)$$

The intersection of two intervals $[x] \cap [y]$ is defined by:

1- if $y^+ < x^-$ or $x^+ < y^-$ the intersection is empty set:

$$[x] \cap [y] = \emptyset \quad (10)$$

2- Otherwise:

$$[x] \cap [y] = [\max\{x^-, y^-\}, \min\{x^+, y^+\}] \quad (11)$$

In the latter case, the union of $[x]$ and $[y]$ is also an interval:

$$[x] \cup [y] = [\min\{x^-, y^-\}, \max\{x^+, y^+\}] \quad (12)$$

When $[x] \cap [y] = \emptyset$, the union of the two intervals is not an interval. For that, the interval hull is defined:

$$[x] \sqcup [y] = [\min\{x^-, y^-\}, \max\{x^+, y^+\}] \quad (13)$$

it is verified that: $[x] \cup [y] \subseteq [x] \sqcup [y]$ for any two intervals $[x]$ and $[y]$.

2.3. Interval systems

Definition II.1 *Parametric uncertain systems can be modelled by interval systems. A SISO interval system that defines a family of systems is denoted $[G](s, [p], [q])$ and is given by:*

$$[G](s, [p], [q]) = \frac{\sum_{j=0}^m [q_j] s^j}{\sum_{i=0}^n [p_i] s^i} = \left\{ \frac{\sum_{j=0}^m p_j s^j}{\sum_{i=0}^n p_i s^i} \mid p_i \in [p_i^-, p_i^+], p_j \in [p_j^-, p_j^+] \right\} \quad (14)$$

Such as: $[q] = [[q_0], \dots, [q_m]]$ and $[p] = [[p_0], \dots, [p_n]]$ are boxes of interval numbers.

The following lemma and theorem concern the performances of two interval systems and are due to [22]. Consider two interval systems having the same structure (orders):

$$[G_1](s) = \frac{\sum_{j=0}^m [b_{1j}] s^j}{\sum_{i=0}^n [a_{1i}] s^i} \quad (15)$$

and

$$[G_2](s) = \frac{\sum_{l=0}^m [b_{2l}] \cdot s^l}{\sum_{k=0}^n [a_{2k}] \cdot s^k} \quad (16)$$

Lemma II.1 *(Inclusion of two interval systems)*

$$\text{if } \begin{cases} [a_{1k}] \subseteq [a_{2k}], \quad \forall k = 1 \dots n \\ \text{and} \\ [b_{1l}] \subseteq [b_{2l}], \quad \forall l = 1 \dots m \end{cases}$$

$$\Rightarrow [G_1](s) \subseteq [G_2](s);$$

Theorem II.1 *(Performances inclusion theorem)*

$$\text{if } [G_1](s) \subseteq [G_2](s);$$

$$\Rightarrow \begin{cases} [g_1](t) \subseteq [g_2](t) \quad \forall t \\ \begin{cases} [\rho]([G_1](j\omega)) \subseteq [\rho]([G_2](j\omega)) \\ [\varphi]([G_1](j\omega)) \subseteq [\varphi]([G_2](j\omega)) \end{cases} \quad \forall \omega \end{cases}$$

where $[g_i](t)$ is the (temporal) impulse response of system $[G_i](s)$, $[\rho]([G_i](j\omega))$ is its modulus and $[\varphi]([G_i](j\omega))$ is its phase.

Proof II.1 See [22].

Theorem II.1 states that if $[G_1](s)$ is included in $[G_2](s)$, its temporal response (impulse response, step response, etc.) will be included in that of $[G_2](s)$. The same holds for the frequential response (bode, nyquist, black-nichols). Such inclusion of responses directly induces the performances inclusion and can be used to design a robust controller as we propose in this paper.

III. Problem statement

Consider an interval system $[G](s, [a], [b])$ to be controlled by a *RST* controller (Fig. 1). The problem consists in finding the different polynomials R , S and T of the controller that

ensures some given performances for the closed-loop $[H_{cl}](s, [a], [b])$ (see Fig. 1) whatever the parameters a and b ranging in $[a]$ and $[b]$ respectively. The main reason of this choice of the *RST* controller is that it is the more general controller structure*.

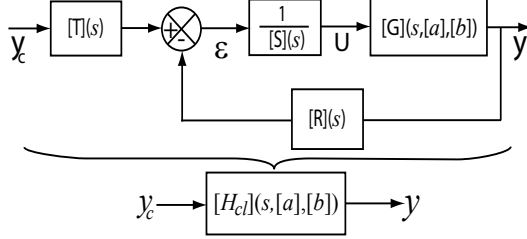


Fig. 1. Closed-loop transfer $[H_{cl}](s, [a], [b])$.

In the sequel, the system $[G](s, [a], [b])$ will be denoted by:

$$[G](s, [a], [b]) = \frac{[N](s, [b])}{[D](s, [a])} \quad (17)$$

where $[N](s, [b])$ and $[D](s, [a])$ are interval polynomials defined by:

$$[N](s, [b]) = 1 + \sum_{j=1}^m [b_j] s^j$$

$$[D](s, [a]) = \sum_{i=0}^n [a_i] s^i$$

Such as $[a] = [[a_0], \dots, [a_n]]$, $[b] = [1, [b_1], \dots, [b_m]]$ and $m \leq n$.

Consider the following performances that we expect for the closed-loop:

- no overshoot.
- settling time $tr_{5\%} \in [tr^-, tr^+]$.
- static error $|\varepsilon| \leq \eta$

These specifications can be easily described by means of an interval model called interval reference model denoted $[H](s)$:

$$[H](s) = \frac{[K_e]}{1 + [\tau]s} \quad (18)$$

where $[\tau] = [\tau^-, \tau^+]$, $[K_e] = [K_e^-, K_e^+]$.

Settling time and static error of (18) are defined by $[tr_{5\%}] = 3 \cdot [\tau]$ and $|\varepsilon| = |[K_e] - 1|$ respectively.

*The PID controller is a particular case of the *RST* controller when $R(s) = T(s)$.

Based on Theorem II.1, the following problem is therefore addressed.

Problem III.1 Given an interval system $[G](s)$ and an interval reference model $[H](s)$ that defines some given performances, find a controller $[C](s)$ such that $[H_{cl}](s) \subseteq [H](s)$. In other words, the problem consists in finding a set of controllers $C(s)$, gathered in an interval $[C](s)$, such that the performances of the closed-loop $[H_{cl}](s)$ are included in the specified performances.

3.1. Computation of the closed-loop model $[H_{cl}](s)$

Let us define fixed-order *RST* structure with a fixed and low degree for each interval polynomials $[R]$, $[S]$ and $[T]$. Polynomials with first-degree are chosen:

$$\begin{aligned} [R](s) &= [r_1]s + [r_0] \\ [S](s) &= [s_1]s + [s_0] \\ [T](s) &= [t_1]s + 1 \end{aligned} \quad (19)$$

Remark III.1 If further we cannot find a controller $[C](s)$ that satisfies Problem III.1, the degree of one or more of the polynomials $[R]$, $[S]$ and $[T]$ can be increased and the controller synthesis is performed again.

Let us define the box of the controller parameters $[\theta] = [[t_1], [r_1], [r_0], [s_1], [s_0]]$.

From Fig. 1, and from the interval system (17) and the controller *RST* (19), the interval closed-loop transfer $[H_{cl}](s, [a], [b], [\theta])$ is given by:

$$[H_{cl}](s, [a], [b], [\theta]) = \frac{[T](s)}{\frac{[S](s)}{[G](s, [a], [b])} + [R](s)} \quad (20)$$

(20) can be rewritten as follows:

$$[H_{cl}](s, [a], [b], [\theta]) = \frac{[T](s) \cdot [N](s, [b])}{[S](s) \cdot [D](s, [a]) + [R](s) \cdot [N](s, [b])} \quad (21)$$

After replacing the different polynomials, we obtain the interval closed-loop transfer $[H_{cl}](s, [a], [b], [\theta])$:

$$[H_{cl}](s, [a], [b], [\theta]) = \frac{([t_1]s + 1)(1 + \sum_{j=1}^m [b_j]s^j)}{([s_1]s + [s_0]) \sum_{i=0}^n [a_i]s^i + ([r_1]s + [r_0])(1 + \sum_{j=1}^m [b_j]s^j)} \quad (22)$$

After developing (22), we obtain:

$$[H_{cl}](s, [p], [q]) = \frac{1 + \sum_{j=1}^e [q_j] s^j}{\sum_{i=0}^r [p_i] s^i} \quad (23)$$

Where $e = m + 1$ and $r = n + 1$. The boxes of interval parameters $[p]$ and $[q]$ are function of the boxes $[a]$, $[b]$ and $[\theta]$.

3.2. Controller derivation

The main objective consists to find the set Θ of the controller parameters vector for which robust performances hold:

$$\Theta := \{\theta \in [\theta] \mid [H_{cl}](s, [p], [q]) \subseteq [H](s)\} \quad (24)$$

This computation of Θ is feasible if and only if $[H_{cl}](s, [p], [q])$ has the same structure than $[H](s)$, i.e. their numerators have the same degree and the same holds for their denominators. As the structure of $[H_{cl}](s, [p], [q])$ is *a priori* fixed, we should adjust the structure of $[H](s)$ to satisfy such condition if it was not yet the case. For that, first let us have a look on the structure of $[H_{cl}](s, [p], [q])$ as in (23). The degree of the numerator is $(m + 1)$ while it is $(n + 1)$ for the denominator. Let us now adjust the structure of $[H](s)$ (see (18)) in order to have the same structure by adding some zeros and poles far away from the imaginary axe. Therefore, we use as reference model:

$$[H](s) = \frac{(1 + \frac{[\tau]}{\kappa} s)^{m+1}}{\frac{1}{[K_e]} \cdot (1 + [\tau] s) (1 + \frac{[\tau]}{\kappa} s)^n} \quad (25)$$

With $\kappa \gg 1$.

After developping (25), we have:

$$[H](s, [w], [x]) = \frac{1 + \sum_{j=1}^{m+1} [x_j] s^j}{\sum_{i=0}^{n+1} [w_i] s^i} \quad (26)$$

Where $[x_j]$ and $[w_i]$ (for $j = 1, \dots, m + 1$ and $i = 0, \dots, n + 1$) are functions of the interval parameters $[K_e]$, $[\tau]$ and the real number κ .

3.3. Inclusion condition

The research of parameter Θ in (24) of the controller is done by using the inclusion $[H_{cl}](s) \subseteq [H](s)$ (see Problem III.1). However, according to Lemma II.1, such inclusion can be satisfied by considering the inclusion of each parameter of $[H_{cl}](s)$ inside that of $[H](s)$. Thus, by using (23) and (26), the problem becomes the research of the controller parameters under the following constraint:

$$\begin{aligned} [q_j] &\subseteq [x_j], \forall j = 1, \dots, m + 1 \\ [p_i] &\subseteq [w_i], \forall i = 0, \dots, n + 1 \end{aligned} \quad (27)$$

and therefore, the computation problem in (24) of the set parameters Θ is reduced to the following problem:

$$\Theta := \left\{ \theta \in [\theta] \mid \begin{aligned} &[q_j](\theta) \subseteq [x_j], \forall j = 1, \dots, m + 1 \\ &[p_i](\theta) \subseteq [w_i], \forall i = 0, \dots, n + 1 \end{aligned} \right\} \quad (28)$$

This problem is known as a *Set-Inversion Problem* which can be solved using interval techniques [3, 14]. The set inversion operation consists to compute the reciprocal image of a compact set called subpaving. The set-inversion algorithm SIVIA (more details are given in [3, 24]) allows to approximate with subpavings the set solution Θ described in (28). This approximation is realized with an inner and outer subpavings, respectively $\underline{\Theta}$ and $\overline{\Theta}$, such that $\underline{\Theta} \subseteq \Theta \subseteq \overline{\Theta}$. The subpaving $\underline{\Theta}$ corresponds to the controller parameter vector for which the problem (28) holds. If $\overline{\Theta} = \emptyset$, then it is guaranteed that no solution exists for (28).

We give in Fig. 2 a flow chart that describes the recursive SIVIA algorithm allowing to solve the problem (28) with guaranteed solutions. SIVIA algorithm requires a search box $[\theta_0]$ (possibly very large) called initial box to which $\overline{\Theta}$ is guaranteed to belong. The inner and outer subpavings ($\underline{\Theta}$ and $\overline{\Theta}$) are initially empty.

Remark III.2 *In the most cases, we are interested to compute an inner subpaving $\underline{\Theta}$ for which we are sure that $\underline{\Theta}$ is included in the set solution Θ , i.e. $\underline{\Theta} \subseteq \Theta$, but when no inner subpaving exists i.e. $\underline{\Theta} = \emptyset$, it is possible to choose parameters inside the outer subpaving, i.e. choose $\theta \in \overline{\Theta}$.*

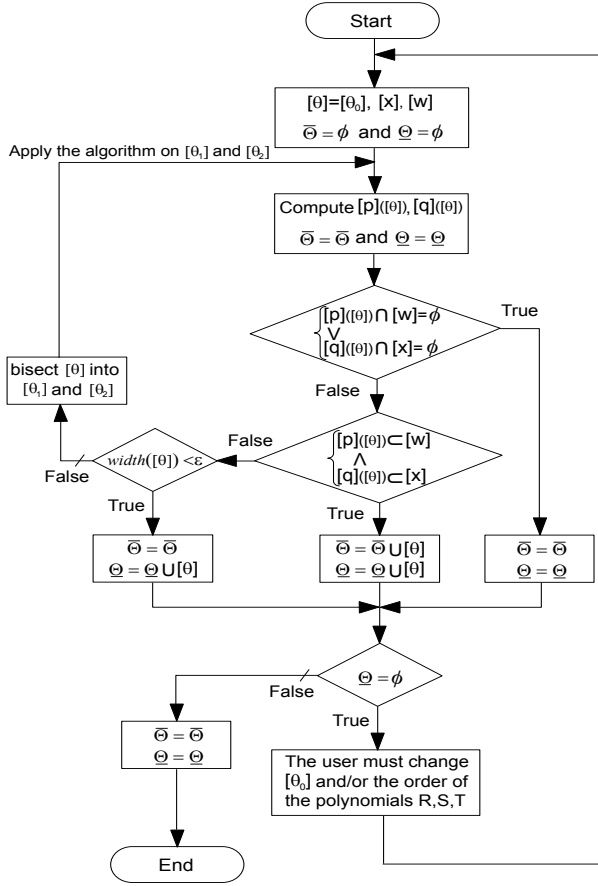


Fig. 2. Algorithm SIVIA used to solve the set-inversion problem (28) [3, 24].

IV. Application to piezocantilevers

In this section, we apply the proposed method to control the deflection of piezoelectric actuators used in microgrippers. These microgrippers are widely used in micromanipulation and microassembly tasks where the required performances are severe (submicrometric accuracy, tens of milliseconds of settling time, no overshoot, etc.) [25]. More precisely, a microgripper is based on two piezoelectric cantilevers also called microactuators or piezocantilever [26, 27]. While one piezocantilever is controlled on position (deflection), the second one is controlled on force. This allows to precisely position a manipulated small object by controlling at the same time the handling force. In this work, we focus our study to the control of the position. The piezocantilever used during the experiments is a unimorph piezocantilever with rectangular cross-section. Such

cantilever is made up of one piezoelectric layer and one passive layer. When a voltage U is applied to the piezolayer, it contracts/expands accordingly to the direction of the applied electric field. As the piezolayer and the passive layer are glued, a global deflection y of the structure is yielded (Fig. 3).

Due to their small sizes, piezocantilevers are very sensitive to environment (thermal variation, vibration, surrounding surface forces, etc.) and to the manipulated objects. This high sensitivity leads to a change of their behavior during the tasks (manipulation, etc.). Unfortunately, the change of the environment is hardly known and hardly modelisable at the micro/nano-scale making impossible the use of a kind of real-time adaptive control law. Beyond, this difficulty is confirmed by the lack of convenient sensors that can be used to measure the environment variation at this scale. This is why it is more attractive to employ more simplified models and to synthesize robust control laws for piezocantilevers. Classical H_∞ robust control laws have successfully been used in our previous works [28], however the orders of the derived controllers were high and may not be convenient for embedded microsystems such as embedded microgrippers. Controllers that account eventual nonlinearities were also used but they required the use of precise models of these nonlinearities [29, 30] which finally make complex the controller implementation. The technique presented in this paper is thus used. Its advantages are 1) the ease of modeling the parametric uncertainties by just bounding them with intervals, 2) and the derivation of a low order controller since its structure is *a priori* fixed.

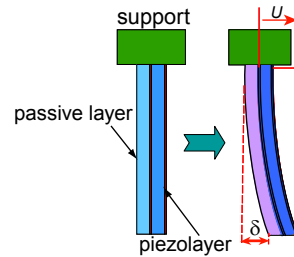


Fig. 3. Principle of a unimorph piezocantilever.

An interval model can be built using two models with scalar parameters. These two point models represent the bounds of the interval

model. In our case, it is impossible to characterize the model variation of a given piezocantilever during its functioning. To derive an interval model $[G](s, [a], [b])$ for piezocantilevers, we use the following procedure :

We have a stock of piezocantilevers with approximately the same dimensions. However, it has been shown that the dynamical model representing the deflection behavior of piezocantilevers respect to the voltage input depends on their dimensional characteristics. Indeed, even if these piezocantilevers have the same global dimensions, there are always small differences of some microns due to the imprecision of the microfabrication process. These small differences yield non-negligible differences on their behaviors and therefore on their models parameters. For that, let us taken any two piezocantilevers of the set of our stock. The two models of the chosen piezocantilevers will be used to derive the interval model $[G](s, [a], [b])$. In order to include the most of the remaining piezocantilevers models, the interval parameters of $[G](s, [a], [b])$ must be expanded. Then, the resulting interval model is used to compute a controller ensuring performances for not only the two used piezocantilevers but for a large set of piezocantilevers.

4.1. Presentation of the setup

Fig. 4 presents the experimental setup. It is composed of:

- two unimorph piezocantilevers. Each piezocantilever is based on a PZT (lead zirconate titanate) for the piezolayer and on copper for the passive layer. The dimensions of the cantilevers are approximately $L \times b \times h = 15mm \times 2mm \times 0.3mm$, where the thicknesses are $0.2mm$ and $0.1mm$ for the PZT and for the Copper respectively,
- an optical sensor (Keyence LC-242) used to measure the deflection of the piezocantilevers. The sensor has $10nm$ of resolution,
- a computer-DSPACE hardware combined with the Matlab-Simulink software for the implementation of the controller and for data acquisition,
- and a high voltage (HV: $\pm 200V$) amplifier used to amplify the input voltage from the computer-DSPACE material.

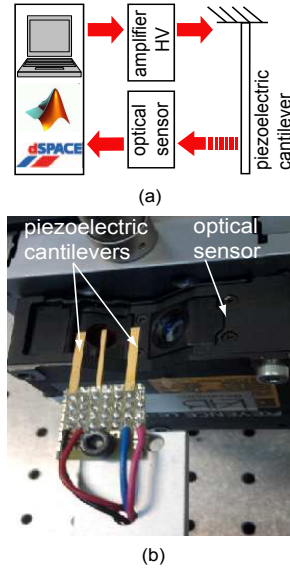


Fig. 4. The experimental setup: piezocantilever controlled through computer DSpace material.

4.2. Modeling of the two piezocantilevers

The linear relation between the deflection at the tip of the piezocantilever and the applied input voltage U is:

$$\delta = G(s)U \quad (29)$$

To identify the two models $G_1(s)$ and $G_2(s)$ corresponding to the two piezocantilevers, a step response is used. A second order was chosen for the model of each piezocantilever because of its sufficiency to account the first resonance and its simplicity (relatively low order). The identification of the two models $G_1(s)$ and $G_2(s)$ was afterwards performed using output error method and the matlab software. We obtain:

$$G_1(s) = \frac{8.08 \times 10^{-8}s^2 + 1.809 \times 10^{-4}s + 1}{8.753 \times 10^{-8}s^2 + 5.234 \times 10^{-6}s + 1.283}$$

$$G_2(s) = \frac{6.992 \times 10^{-8}s^2 + 1.807 \times 10^{-4}s + 1}{9.844 \times 10^{-8}s^2 + 5.37 \times 10^{-6}s + 1.448} \quad (30)$$

4.3. Derivation of the interval model

Let us rewrite each model $G_i(s)$ ($i = 1, 2$) as follows:

$$G_i(s) = \frac{b_{2i}s^2 + b_{1i}s + 1}{a_{2i}s^2 + a_{1i}s + a_{0i}} \quad (31)$$

The interval model $[G](s, [a], [b])$ which represents a family of piezocantilever models is derived using the two point models $G_i(s)$. Considering each parameter of $G_1(s)$ and the corresponding parameter in $G_2(s)$ as an endpoint of the interval parameter in $[G](s, [a], [b])$, we have:

$$[G](s, [a], [b]) = \frac{[b_2]s^2 + [b_1]s + 1}{[a_2]s^2 + [a_1]s + [a_0]} \quad (32)$$

such as:

$$\begin{aligned} [b_2] &= [\min(b_{21}, b_{22}), \max(b_{21}, b_{22})] \\ [b_1] &= [\min(b_{11}, b_{12}), \max(b_{11}, b_{12})] \\ [a_2] &= [\min(a_{21}, a_{22}), \max(a_{21}, a_{22})] \\ [a_1] &= [\min(a_{11}, a_{12}), \max(a_{11}, a_{12})] \\ [a_0] &= [\min(a_{01}, a_{02}), \max(a_{01}, a_{02})] \end{aligned}$$

After computation, we obtain:

$$\begin{aligned} [b_2] &= [6.992, 8.08] \times 10^{-8} \\ [b_1] &= [1.807, 1.809] \times 10^{-4} \\ [a_2] &= [8.753, 9.844] \times 10^{-8} \\ [a_1] &= [5.234, 5.37] \times 10^{-6} \\ [a_0] &= [1.283, 1.448] \end{aligned}$$

In order to increase the stability margin of the closed-loop system and to include other piezocantilever models, we propose to extend the interval parameters of model (32). However, if the widths of these interval parameters are too large, it is difficult to find a controller that respects both the stability and performances of the closed-loop. After some trials of controller design, we choose to expand the width of each interval parameter of (32) by 10%. It represents a good compromise between the extension of the width and the possibility to find a robust controller. So, the extended parameters of the interval model which will be used to compute the controller are:

$$\begin{aligned} [b_2] &= [6.937, 8.134] \times 10^{-8} \\ [b_1] &= [1.8067, 1.809] \times 10^{-4} \\ [a_2] &= [8.698, 9.898] \times 10^{-8} \\ [a_1] &= [5.227, 5.376] \times 10^{-6} \\ [a_0] &= [1.274, 1.456] \end{aligned} \quad (33)$$

4.4. Definition of the time specifications

Micromanipulation tasks generally require a submicrometric accuracy and high repeatability. Furthermore, the behavior of piezocantilevers used in microassembly and micromanipulation is

often desired to be without overshoot to ensure better quality tasks and to avoid destroying the manipulated micro-object or conversely to avoid the destruction of the actuators themselves. For all that, we consider the following specifications that correspond to the requirement in micropositioning tasks for microassembly and micromanipulation that use piezoelectric microgrippers:

- behavior without or with small overshoot,
- settling time $tr_{5\%} < 30ms$,
- static error allowed $|\varepsilon| \leq 1\%$.

4.5. Computation of the closed-loop transfer

From the model $[G](s, [a], [b])$ in (32) and from the RST controller in (19) to be designed, we derive the closed-loop $[H_{cl}](s, [a], [b], [\theta])$:

$$[H_{cl}](s, [a], [b], [\theta]) = \frac{([t_1]s + 1)([b_2]s^2 + [b_1]s + 1)}{([s_1]s + [s_0])([a_2]s^2 + [a_1]s + 1) + ([r_1]s + [r_0])([b_2]s^2 + [b_1]s + 1)} \quad (34)$$

After developing (34), the closed-loop can be written as follows:

$$[H_{cl}](s, [p], [q]) = \frac{[q_3]s^3 + [q_2]s^2 + [q_1]s + 1}{[p_3]s^3 + [p_2]s^2 + [p_1]s + [p_0]} \quad (35)$$

Where the boxes $[q]$, $[p]$ depend on the boxes $[a]$ and $[b]$ of the interval model and on the interval parameters $[\theta] = [[t_1], [r_0], [r_1], [s_1], [s_0]]$ of the controller as follows:

$$\begin{aligned} [q_3] &= [t_1][b_2] \\ [q_2] &= [t_1][b_1] + [b_2] \\ [q_1] &= [t_1] + [b_1] \\ [p_3] &= [s_1][a_2] + [r_1][b_2] \\ [p_2] &= [s_1][a_1] + [s_0][a_2] + [r_1][b_1] + [r_0][b_2] \\ [p_1] &= [s_1][a_0] + [s_0][a_1] + [r_0][b_1] + [r_1] \\ [p_0] &= [s_0][a_0] + [r_0] \end{aligned} \quad (36)$$

4.6. Computation of the interval reference model

Specifications that define the desired behavior of the closed-loop can be easily described by means of an interval reference model. According to the required specifications given in Section 4.4 and

according to the structure of the closed-loop (35), the interval reference model (derived from (25)) must have $n = m = 2$. Thus:

$$[H](s) = \frac{(1 + \frac{[\tau]}{\kappa}s)^3}{\frac{1}{[K_e]} \cdot (1 + [\tau]s)(1 + \frac{[\tau]}{\kappa}s)^2} \quad (37)$$

Such as $[\tau] = [0, 10ms]$, $[K_e] = [0.99, 1.01]$ and $\kappa = 10$.

After developping (37), we obtain:

$$[H](s) = \frac{[x_3]s^3 + [x_2]s^2 + [x_1]s + 1}{[w_3]s^3 + [w_2]s^2 + [w_1]s + [w_0]} \quad (38)$$

Where the boxes $[x]$ and $[w]$ are function of the box $[[K_e], [\tau], [\kappa]]$ as follows:

$$\begin{aligned} [x_3] &= \frac{\tau^3}{\kappa^3} \\ [x_2] &= \frac{3\tau^2}{\kappa^2} \\ [x_1] &= \frac{3\tau}{\kappa} \\ [w_3] &= \frac{\tau^3}{\kappa^2 K_e} \\ [w_2] &= \frac{(1 + 2\kappa)\tau^2}{\kappa^2 K_e} \\ [w_1] &= \frac{(\kappa + 2)\tau}{\kappa K_e} \\ [w_0] &= \frac{1}{K_e} \end{aligned} \quad (39)$$

4.7. Derivation of the controller

The derivation of the controller consists to find the set (or subset) of the interval parameters $[\theta] = [[t_1], [r_0], [r_1], [s_1], [s_0]]$ for which specifications hold, i.e. find $[\Theta]$ such as:

$$\Theta := \left\{ \theta \in [\theta] \mid \begin{aligned} &[q_j](\theta) \subseteq [x_j], \forall j = 1, \dots, 3 \\ &[p_i](\theta) \subseteq [w_i], \forall i = 0, \dots, 3 \end{aligned} \right\} \quad (40)$$

where $[[p_i], [q_j]]$ and $[[w_i], [x_j]]$ (for $i = 0 \dots 3$ and $j = 1 \dots 3$) are defined in (36) and (39) respectively.

Remark IV.1 The number of unknown parameters (see (19)) are 5 while the number of inclusions (40) is 7. Therefore, there are more inclusions than unknown variables. So, the set solution Θ is given by the intersection of the set solution of each inclusion in (40) as follows:

$$\Theta = \bigcap_{i=1}^7 (set_sol)_i$$

such as: $(set_sol)_i$ is the set solution of the i^{th} inclusion.

SIVIA algorithm is applied to solve the problem (40) and to characterize the set solution Θ . However, the computation time increases exponentially with the number of the parameters making difficult to solve such problem with multiple parameters. Since our objective is not to compute all possible controllers RST that ensure specifications, but to find a set (or subset) of controllers RST satisfying desired behaviors of the closed-loop (see Section 4.4). For that, we choose to solve the problem (40) not through SIVIA alone but also through some hand-tuning prior the algorithmic solution of SIVIA. The procedure of hand-tuning consists to adjust some parameters (fixed as a scalar or as an interval), then to compute the set solution of the remaining parameters thanks to SIVIA.

The three first inclusions $[q_j] \subseteq [x_j]$ for $j = 1 \dots 3$ depend only of the parameter $[t_1]$, so they can be solved independently. These inclusions represent nonlinear system equations with one parameter which can be solved using SIVIA algorithm. After Application of SIVIA, we obtain the following solution:

$$[t_1] = [0, 2.81 \times 10^{-3}] \quad (41)$$

Now, it remains to solve the second part of the inclusions (40), i.e. the inclusions $[p_i] \subseteq [w_i]$ for $i = 0, \dots, 3$. In order to cancel the static error, i.e. $[p_0] = p_0 = 1$, the parameters $[s_0]$ and $[r_0]$ are manually adjusted as follows:

$$\begin{cases} [s_0] = s_0 = 0 \\ [r_0] = r_0 = 1 \end{cases} \quad (42)$$

which confirms that the last inclusion $[p_0] \subseteq [w_0]$ is respected.

Finally, we have to solve the following problem with two parameters $[s_1]$ and $[r_1]$:

$$\begin{aligned} [s_1][a_2] + [r_1][b_2] &\subseteq \frac{\tau^3}{\kappa^2 K_e} \\ [s_1][a_1] + [r_1][b_1] + [b_2] &\subseteq \frac{1 + 2\kappa}{\kappa^2} \frac{\tau^2}{K_e} \\ [s_1][a_0] + [b_1] + [r_1] &\subseteq \frac{\kappa + 2}{\kappa} \frac{\tau}{K_e} \end{aligned} \quad (43)$$

To characterize the set solution $S_{s_1 r_1}$ of the parameters $[s_1]$ and $[r_1]$, we apply SIVIA algorithm for the second time to the problem of linear system equations (43). We choose an initial box $[s_{10}] \times [r_{10}] = [0.01 \times 10^{-3}, 10 \times 10^{-3}] \times [0.01 \times 10^{-3}, 10 \times 10^{-3}]$ and accuracy of $\epsilon = 0.1 \times 10^{-3}$. The obtained subpaving is given in Fig. 5.

The area in blue corresponds to the inner subpaving $\underline{S}_{s_1 r_1}$ i.e. the set solution $[s_1] \times [r_1]$ of the linear system equations (43). The area in white corresponds to the outer subpaving $\overline{S}_{s_1 r_1}$, it contains the boxes for which no decision on the test of inclusion in (43) can be taken. $\overline{S}_{s_1 r_1}$ can be minimized by increasing the computation accuracy. The boxes in red correspond to the parameters $[s_1]$ and $[r_1]$ for which the inclusions (43) do not hold, i.e. the intersection between the left and right terms of (43) is empty. A controller with the parameters $t_1 \in [0, 2.8 \times 10^{-3}]$, $s_0 = 0$, $r_0 = 1$ and any choice of s_1 , r_1 in the blue colored area $\underline{S}_{s_1 r_1}$ satisfies the required performances specified in Section 4.4 for the interval system (uncertain system) $[G](s, [a], [b])$ with parameters given in (33).

Note that the set $\underline{S}_{s_1 r_1}$ does not represent the set of all possible controllers that satisfy the required performances but a subset of these controllers. Therefore, any change in the values of the parameters $[s_0]$ and $[r_0]$ leads to a change in the subset $\underline{S}_{s_1 r_1}$. Thus, a choice of the parameters s_1 and r_1 inside the red area (non-solution set) may satisfy the desired performances because this non-solution set corresponds to the parameters s_1 and r_1 for which the conditions (43) do not hold.

The searched inner subpaving $\underline{\Theta}$ is defined as follows:

$$\underline{\Theta} := \left\{ \begin{array}{l} \theta \in [\theta] | t_1 \in [0, 2.8 \times 10^{-3}], \\ r_1 = 1, s_0 = 0, \{s_1, r_1\} \in \underline{S}_{s_1 r_1} \end{array} \right\} \quad (44)$$

For the implementation, we choose the following polynomials for the *RST* controller:

$$\begin{aligned} R(s) &= 0.5 \times 10^{-3}s + 1 \\ S(s) &= 5 \times 10^{-3}s \\ T(s) &= 1 \times 10^{-5}s + 1 \end{aligned} \quad (45)$$

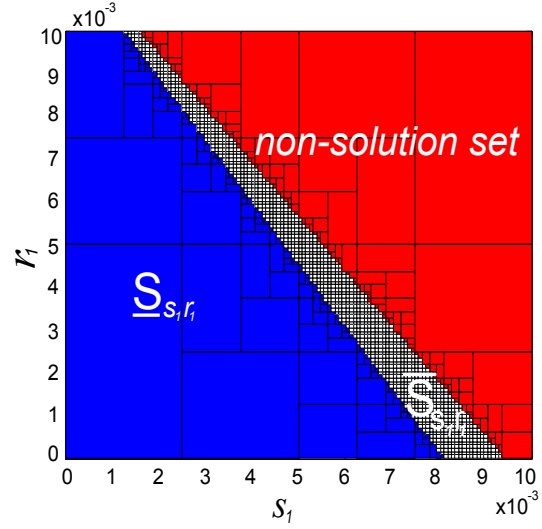


Fig. 5. Resulting subpaving $[s_1] \times [r_1]$

V. Controller implementation and experimental results

5.1. Controller implementation

This part consists to apply the RST controller (45) to control the deflection of the piezocantilevers. For that, the closed-loop control structure in Fig. 1 is transformed as in Fig. 6 to have a causal controller:

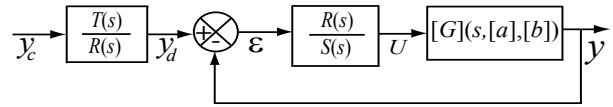


Fig. 6. Loop control with RST.

5.2. Experimental result

Fig. 7 presents the experimental results when a step reference input $y_c = 20\mu m$ is applied. As shown on Fig. 7, the computed controller has played its role. Indeed the experimental behavior of the closed-loop (tested on the two piezocantilevers) is without overshoot, with settling times $tr_1 = 19.5ms \leq 30ms$, $tr_2 = 21.5ms \leq 30ms$ respectively for the piezocantilevers 1 and 2 and finally the static errors remain bounded by the specified interval.

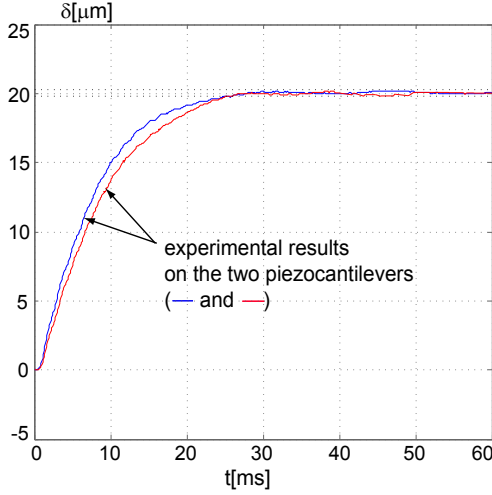


Fig. 7. Step responses envelope compared with the experimental results.

VI. Closed-loop stability analysis

In this section, we present a robust stability result of the closed-loop systems with the designed RST controller (Fig. 6). This analysis stability is done analytically and graphically. As the computed transfer $\frac{T(s)}{R(s)}$ is stable, the check the robust stability of the looped interval system with the implemented RST controller can be reduced to the check of the stability of the the interval transfert that relates the output y to the input signal y_d .

The stability analysis of an interval system is based on the roots of the so-called characteristic polynomial. This polynomial corresponds to the denominator of the interval closed-loop system. The interval closed-loop system is stable if and only if all the roots of the characteristic polynomial are in the left part \mathbb{C}^- of the complex plane, i.e. they have strictly negative parts.

The characteristic polynomial of the transfert from the input signal y_d to the output y is defined as follows :

$$[P](s) = [p_3]s^3 + [p_2]s^2 + [p_1]s + 1 \quad (46)$$

Such as: $[p_3] = [a_2]s_1 + [b_2]r_1$, $[p_2] = [b_2] + [a_1]s_1 + r_1[b_1]$, $[p_1] = [b_1] + r_1 + [a_0]s_1$.

$r_1 = 0.5 \times 10^{-3}$ and $s_1 = 5 \times 10^{-3}$ are the parameters of the implemented polynomials $R(s)$ and $S(s)$ (45).

According to the Routh's criterion, all the roots of the interval polynomial $[P](s)$ are in the

left part \mathbb{C}^- if and only if the following conditions are satisfied:

$$\begin{aligned} [p_3] &> 0 \\ [p_2] &> 0 \\ [p_1] &> 0 \\ [p_2][p_1] - [p_3] &> 0 \end{aligned} \quad (47)$$

After computation, we obtain:

$$\begin{aligned} [p_3] &= [4.696, 5.355] \times 10^{-10} > 0 \\ [p_2] &= [1.597, 1.7418] \times 10^{-7} > 0 \\ [p_1] &= [7.054, 7.962] \times 10^{-3} > 0 \\ [p_2][p_1] - [p_3] &= [5.951, 8.981] \times 10^{-10} > 0 \end{aligned} \quad (48)$$

As all the terms in (48) are strictly positive, the implemented controller ensure the robust stability whatever a given system G including in the interval system $[G](s, [a], [b])$, i.e. $\forall G \in [G](s, [a], [b])$.

It is also possible to study the δ -stability of our feedback interval systems. The check of the δ -stability can be defined by the check of the usual stability but instead of the Laplace variable s , we use $s - \delta$ ($\delta > 0$). The interval polynomial $[P](s)$ is δ -stability if and only if all its roots are in the part Γ_δ of complex plane located on the left of the vertical line $Re(s) = -\delta$. For that, we compute the maximal δ for which the implemented RST controller ensures the δ -stability for the interval system $[G](s, [a], [b])$. We can rewrite $[P](s - \delta)$ as follows:

$$[P](s - \delta) = \alpha_3 s^3 + \alpha_2 s^2 + \alpha_1 s + \alpha_0 \quad (49)$$

where:

$$\begin{aligned} \alpha_3 &= [p_3], & \alpha_2 &= [p_2] - 3\delta[p_3], & \alpha_1 &= [p_1] - 2\delta[p_2] - 3\delta^2[p_3] \\ \alpha_0 &= 1 - \delta[p_1] + \delta^2[p_2] + 3\delta^3[p_3]. \end{aligned}$$

The polynomial $[P](s - \delta)$ is stable if and only if:

$$\begin{aligned} [\alpha_3] &> 0 \\ [\alpha_2] &> 0 \\ [\alpha_1] &> 0 \\ [\alpha_2][\alpha_1] - [\alpha_3][\alpha_0] &> 0 \end{aligned} \quad (50)$$

The resolution of this nonlinear inequalities problem leads to the admissible values of δ that satisfy the inequalities (50). After computation, we obtain the set interval of the parameter δ :

$$\delta = [0, 30.493] \quad (51)$$

Finally, we can conclude that the implemented RST controller ensures the δ -stability for the interval system whatever δ less than 30.493.

In order to assess the stability margins, we study the Black-Nichols diagram of the open-loop system $[L](s)$ (Fig. 6) defined by:

$$[L](s) = \frac{R(s)}{S(s)} [G](s, [a], [b]) \quad (52)$$

Indeed, a stability margin is a quantity that characterizes the distance of the curve of Black-Nichols from the critical point $(-180, 0dB)$. The stability margins analysis allows to study the robustness of an enslavement or of a controller. This analysis is based on two parameters: gain and phase margins which are measures of stability for a feedback system.

Fig. 8 presents the Black-Nichols diagram of the open-loop system $[L](s)$ and that of the controlled system $[G](s, [a], [b])$.

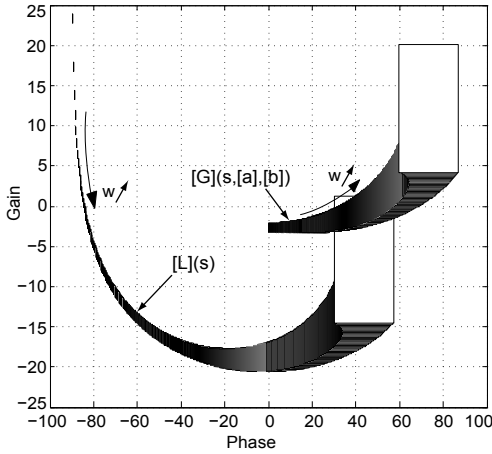


Fig. 8. Black-Nichols diagrams of the open-loop system $[L](s)$ and the interval system $[G](s, [a], [b])$.

As seen on the figure, the obtained phase and gain margins with the implemented RST controller are $M\varphi \approx 95$ (at a pulsation about 150Hz) and $MG = \infty$ respectively. The obtained results on the stability analysis in this section prove the robustness of the RST controller and the efficiency of the proposed method to design robust controller.

VII. Conclusion

In this paper, a method to design robust controllers for systems with uncertain parameters has been proposed. While the uncertain parameters are described by intervals, the controller structure is given *a priori* (a fixed-order RST controller). The main advantages of the proposed approach are therefore the natural way to model the uncertainties and the derivation of a low order controller. Starting from specified performances, the calculation of the controller parameters is formulated as a set-inversion problem that can be solved using existing algorithm. Experimental tests of the proposed method were carried out on piezoelectric actuators. The experimental results showed its efficiency. A stability analysis of the closed-loop system confirms the robustness of the computed controller.

REFERENCES

1. Barmish B R. 1994. 'New Tools for Robustness of Linear Systems', Macmillan, New York, USA.
2. Dasgupta S, Anderson B D O., Chockalingam G, Fu M. 1994. 'Lyapunov functions for uncertain systems with applications to the stability of time varying systems', IEEE Trans. on Circuits and Systems, vol.41, pp.93-106.
3. Jaulin L, Kieffer M, Didrit O, Walter E. 2001. 'Applied Interval Analysis', Springer.
4. Bondia J, Kieffer M, Walter E, Monreal J, Picò J. 2004. 'Guaranteed tuning of PID controllers for parametric uncertain systems', IEEE CDC, 2948-2953.
5. Dullerud G E, Paganini F G. 2000. 'A course in robust control theory: a convex approach', 1st edition, Springer.
6. Reza Moheimani S O. 2001. 'Perspectives in Robust Control', 1st edition, Springer.
7. Ur Rehman O, Fidan B, Petersen I. 2011. 'Uncertainty modeling and robust minimax LQR control of multivariable nonlinear systems with application to hypersonic flight', Asian Journal of Control, DOI: 10.1002/asjc.399.
8. Sadeghzadeh A. 2011. 'Identification and robust control for systems with ellipsoidal parametric uncertainty by convex optimization', Asian Journal of Control, DOI: 10.1002/asjc.437.
9. Chen W, Zhang Z. 2011. 'Nonlinear adaptive learning control for unknown time-varying parameters and unknown time-varying

- delays', Asian Journal of Control, DOI: 10.1002/asjc.403.
10. Liu Y J, Tong S C, Li T S. 2010. 'Adaptive fuzzy controller design with observer for a class of uncertain nonlinear MIMO systems', Asian Journal of Control, DOI: 10.1002/asjc.214.
 11. Wang C. 2010. 'New delay-dependent stability criteria for descriptor systems with interval time delay', Asian Journal of Control, DOI: 10.1002/asjc.287.
 12. Banjerdpongchai D, How J P. 1997. 'LMI Synthesis of Parametric Robust H_∞ Controllers', In Proceeding of the American Control Conference, pp.493-498.
 13. Balas G J, Doyle J C, Glover K, Packard A, Smith R. 1993. ' μ -Analysis and Synthesis Toolbox', The Mathworks Inc.
 14. Moore R E. 1966. 'Interval analysis', Prentice-Hall, Englewood Cliffs N. J.
 15. Kharitonov V L. 1978. 'Asymptotic stability of an equilibrium position of a family of systems of linear differential equations'. Differential'nye Uravneniya, 14, 2086-2088.
 16. Walter E, Jaulin L. 1994. 'Guaranteed characterization of stability domains via set inversion', IEEE Trans. on Autom. Control, 39(4), 886-889.
 17. Smagina Y, Brewerb I. 2002. 'Using interval arithmetic for robust state feedback design', Systems and Control Letters, 187-194.
 18. Chen C T, Wang M. D. 1997. 'Robust controller design for interval process systems'. Computers & Chemical Engineering, 21, 739-750.
 19. Li K, Zhang Y. 2009. 'Interval Model Control of Consumable Double-Electrode Gas Metal Arc Welding Process', IEEE - Trans. on Automation Science and Engineering (T-ASE), 1-14.
 20. Chen C T, Wang M D. 2000. 'A two-degrees-of-freedom design methodology for interval process systems', Computers and Chemical Engineering, 23, 1745-1751.
 21. Bondia J, Picò J. 2003. 'A geometric approach to robust performance of parametric uncertain systems', International Journal of Robust and Nonlinear Control, vol. 13, 1271-1283.
 22. Rakotondrabe M, 2011. 'Performances inclusion for stable interval systems', IEEE - ACC, proceedings, San Fransisco CA USA.
 23. Khadraoui S, Rakotondrabe M, Lutz P. 2010. 'Robust control for a class of interval model: application to the force control of piezoelectric cantilevers', IEEE - CDC, pp.4257-4262, Atlanta Georgia USA.
 24. Jaulin L, Walter E. 1993. 'Set inversion via interval analysis for nonlinear bounded-error estimation', Automatica, 29(4), 1053-1064.
 25. Bargiel S, Rabenoroso K, Clevy C, Gorecki C, Lutz P. 2010. 'Towards Micro-Assembly of Hybrid MOEMS Components on Reconfigurable Silicon Free-Space Micro-Optical Bench', Journal of Micromechanics and Microeng., 20(4).
 26. Haddab Y, Chaillet N, and Bourjault A. 2000. 'A microgripper using smart piezoelectric actuators', IEEE/RSJ International Conference on Intelligent Robot and Systems (IROS), Takamatsu - Japan, 1, 659-664.
 27. Agnus J, Breguet J M, Chaillet N, Cois O, De Lit P, Ferreira A, Melchior P, Pellet C, Sabatier J. 2003. 'A smart microrobot on chip: design, identification and modeling', IEEE/ASME AIM, Kobe Japan, 685-690.
 28. M. Rakotondrabe, Y. Haddab and P. Lutz, 'Quadrilateral modelling and robust control of a nonlinear piezoelectric cantilever', IEEE - Trans. on Control Systems Technology, 17(3), pp:528-539, May 2009.
 29. Yi-Chen Huang and De-Yao Lin, 'Ultra-fine tracking control on piezoelectric actuated motion stage using piezoelectric hysteretic model', Asian Journal of Control, 6(2), p.208-216, 2004.
 30. J-C. Shen, W-Y. Jywe, C-H. Liu, Y-T. Jian and J. Yang, 'Sliding-mode control of a three-degrees-of-freedom nanopositioner', Asian Journal of Control, 10(3), p.267-276, 2008.